Nuclear Instruments and Methods in Physics Research B 371 (2016) 278–282

Contents lists available at ScienceDirect

Nuclear Instruments and Methods in Physics Research B

journal homepage: www.elsevier.com/locate/nimb

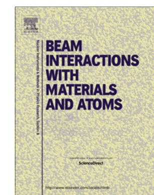

Study of In distribution on GaInSb:Al crystals by ion beam techniques

M. Streicher [a,b,*], V. Corregidor [b], N. Catarino [b], L.C. Alves [c], N. Franco [b], M. Fonseca [d,e], L. Martins [e], E. Alves [b], E.M. Costa [a], B.A. Dedavid [a]

[a] Pontifícia Universidade Católica do Rio Grande do Sul, Av. Ipiranga, 6681, Porto Alegre, RS, Brazil
[b] Instituto de Plasmas e Fusão Nuclear (IPFN), Instituto Superior Técnico, Universidade de Lisboa, E.N. 10, 2695-066 Bobadela LRS, Portugal
[c] Centro de Ciências e Tecnologias Nucleares (C2TN), Instituto Superior Técnico, Universidade de Lisboa, E.N. 10, 2695-066 Bobadela LRS, Portugal
[d] Universidade Europeia, Laureate International Universities, 1500-210 Lisboa, Portugal
[e] Laboratório de Instrumentação, Engenharia Biomédica e Física da Radiação (LIBPhys-UNL), Departamento de Física, FCT-UNL, 2829-516 Monte da Caparica, Portugal

ARTICLE INFO

Article history:
Received 1 July 2015
Received in revised form 10 September 2015
Accepted 10 September 2015
Available online 24 September 2015

Keywords:
Ternary alloy of $Ga_{1-x}In_xSb$
PIXE
PIGE
Composition
Aluminum

ABSTRACT

III–V ternary alloys semiconductor materials, in particular $Ga_{1-x}In_xSb$, are ideal candidates for device substrates because of the possibility to define the lattice constant as a function of the third element, indium. Aluminum, an isoelectric dopant for Ga and In, increases the carrier mobility in GaSb crystals and has influence over the concentration of native defects by passivating and/or compensating them. To understand the influence of Al on the distribution of indium in ternary alloys of $Ga_{0.8}In_{0.2}Sb$, pure and doped ingots were obtained with approximately 10^{20} atoms/cm^3 of Al using a vertical Bridgman system. Analysis by scanning electron microscopy (SEM), energy dispersive X-ray spectrometry (EDX), X-ray diffraction (XRD), particle induced X-ray emission (PIXE) and particle induced gamma ray emission (PIGE) were used to obtain information on the structure defects and chemical composition of the crystals.

The doped ingots showed good structural homogeneity when compared with the undoped alloy, and they were free from cracks and micro cracks. All of the obtained ingots present precipitates, twins and grains with different concentrations of In.

The small compositional variation observed in the doped ingots along the radial direction (measured by PIXE), may be related to the solid–liquid interface's quasi-equilibrium behavior. Regarding to the growth direction, it was observed that the undoped ingots exhibit a higher segregation phenomenon of the third element than the doped ingots.

The obtained results indicate that aluminum influences the indium distribution in the ingots, thus ternary ingots with more homogeneous composition can be obtained and consequently electrical properties improved.

© 2015 Elsevier B.V. All rights reserved.

1. Introduction

Semiconductor alloys that exhibit complete miscibility in both, liquid and solid, state as SiGe, InGaAs, and GaInSb, are of great interest as substrates for micro and optoelectronics, as well as bulk for thermophotovoltaic devices [1–4].

Applications of ternary alloys as substrates are related to the possibility to change the lattice constant as a function of concentration of a third element [4,6,5]. The presence of indium in the $Ga_{1-x}In_xSb$ compounds modifies the lattice parameter of the alloy from 6.09 Å when $x = 0$ (GaSb) to 6.48 Å when $x = 1$ (InSb), and also the bandgap from 0.72 eV ($x = 0$) to 0.18 eV ($x = 1$) [4,6,5]. The use of GaInSb as substrate for the thermophotovoltaic cells necessitates low band gaps, which correspond to $x > 0.2$ [7].

The solid–liquid (S–L) interface shape during growth process, the growth rate and the rejection on the third element towards the melt, are the main factors that make difficult the growth of these ingots with a structural and compositional homogeneity [1,8–16]. In this way, the main challenge to overcome when growing these ternary alloys is the indium segregation, that causes a constitutional supercooling (CSR) due to solute accumulation at S–L interface front [3,17–22].

The Bridgman method is the most suitable growth technique for obtaining large-diameter GaInSb alloys ingots. To grow these ternary ingots, low temperature gradient and low growth rate are required. A low temperature gradient helps to ensure a planar melt–solid interface shape, which is necessary for a uniform radial composition in the ingots as well as reducing the strain level in the

* Corresponding author at: Pontifícia Universidade Católica do Rio Grande do Sul, Av. Ipiranga, 6681, Porto Alegre, RS, Brazil. Tel.: +55 5135089203.
E-mail address: smorgana@gmail.com (M. Streicher).

http://dx.doi.org/10.1016/j.nimb.2015.09.032
0168-583X/© 2015 Elsevier B.V. All rights reserved.

crystal to avoid cracking. Low solidification rate is necessary to avoid constitutional supercooling at solid–liquid interface, which leads to a single-to-dendritic-grain transition and also to the generation of microcracks. It is also known that to avoid the segregation is not easy, and the segregation that settles in front of the solid–liquid interface during the advance of solidification process produces ingots with no uniform spatial composition and hence, with not homogeneous electrical and optical properties [10].

The Bridgman method, in the last years, has been enhanced with modifications such as solidification under microgravity, stirring, magnetic field in melt and submerged baffle. These modifications allowed to a higher quality bulk crystals of $Ga_{1-x}In_xSb$ ternary using the conventional and non-convectional Bridgman method [7,11,12,14,23–31].

In this paper, we propose to explore another possibility of decreasing the segregation of indium in GaInSb alloys with addition of aluminum as doping. Dopants such as tellurium (Te), selenium (Se) and others are used commonly to grow n-type GaSb and InSb crystals. The doping not only has the function to change electrical parameters, but also helps to decrease the native defects, dislocations and others defects. The doping is a factor dictating the crystalline quality and spatial alloy composition in GaSb and InSb ingots [32]. Aluminum has the distribution coefficient $k_o > 1$ and indium $k_o < 1$ in GaInSb [33]. For this reason, the concentration of aluminum decrease and indium increases from the beginning to end of the ingot.

Aluminum is an isoelectronic dopant of GaSb, so it does not change the number of charge carriers, but increases their mobility. It will have preference for gallium sites not only because of valence, but also due to the proximity of atomic radius. Hidalgo et al. [34] in their article on growth and characterization of GaSb:Al ingots, suggest that the presence of aluminum together with indium could passivate extended defects and/or compensate the native defects, although there aren't conclusive studies. Thus, the aim of this paper is to observe the performance of indium segregation at $Ga_{1-x}In_xSb$ and $Ga_{1-x}In_xSb$:Al ingots ($x = 0.2$) obtained through the conventional Bridgman method.

2. Experimental

The $Ga_{0.8}In_{0.2}Sb$ ternary alloys were obtained from polycrystalline GaSb (5 N), InSb (5 N) and Al (4 N). Quartz ampoules with a cone angle of 30° and 12 mm of diameter [35] were used as crucible. After charging, they were closed with a small Argon pressure inside. The initial concentration was defined as $x = 0.2$. First, the synthesis was performed at 800 °C for 12 h [36], after this period the ampoules were moved to the solidification zone of the furnace.

Then, the ingot was remelted at 800 °C for 2 h to homogenize the melt. After this, the temperature in the furnace was reduced to around 100 °C above the melting temperature of the ternary compound $Ga_{0.8}In_{0.2}Sb$ ($T_M \approx 618$ °C). Finally, the growth was performed at a speed of 2.5 mm/h and the temperature gradient on solid/liquid interface was about 3.3 °C/mm [37]. The entire process usually takes one week for each ingot.

The ingots obtained were cut longitudinally to the growth direction for compositional and morphological characterization by energy dispersive spectrometry and scanning electron microscopy (EDS/SEM). Also, wafers were taken perpendicular to the direction of growth (Fig. 1) for structural and compositional characterization by X-ray diffraction (XRD), particle induced X-ray emission (PIXE) and particle induced gamma-ray emission (PIGE). The specimens were chemically polished with colloidal silica and sodium hypochlorite as described in Costa et al. [21] for posterior analysis.

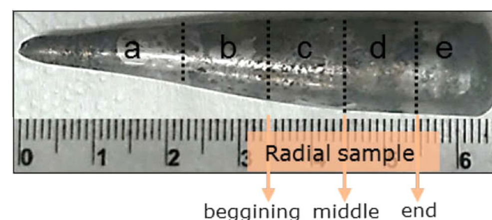

Fig. 1. Image of an ingot highlighting the regions analyzed by EDS/SEM. Radial samples (beginning, middle and end) taken from the body of ingot and analyzed by XRD and IBA techniques are also identified.

EDS/SEM was performed using a FEG Inspect F50 at Laboratório Central de Microscopia Eletrônica – Pontifícia Universidade Católica do Rio Grande do Sul (LabCEMM – PUCRS), in Porto Alegre (Brazil). SEM images in BSE mode were obtained at an acceleration voltage of 20 kV and the X-rays were detected with an Apollo X-EDAX® detector.

Ion beam analyses were made at Campus Tecnológico e Nuclear – Instituto Superior Técnico (CTN-IST), in Lisbon (Portugal). PIXE experiments were made in one of the lines of the 2.5 MV Van de Graaff accelerator, in the chamber dedicated to fusion research. A 2.0 MeV proton beam was collimated to a spot (1 mm in diameter). Measurements were performed at normal incidence. The samples were mounted on a mounting stage aluminum holder with x–y–z sample manipulators. By a combination of sample displacements, the entire sample surface was measured. X-rays were detected with a 30 mm^2 Si(Li) detector (positioned at 150° relative to the beam direction) and a 50 μm thick Mylar filter was used in front of the detector. PIXE spectra were analyzed with GUPIX code [38].

For light element analysis, we used a standard-free method for PIGE in thick samples, based on the ERYA code – Emitted Radiation Yield Analysis, that integrates the nuclear reaction excitation function along the depth of the sample [39]. PIGE experiments were carried out in the nuclear reaction beam line of the 3 MV Tandem accelerator at CTN-IST, using a proton beam with 3.040 MeV energy, which corresponds to a non-resonant region, in order to integrate the cross section values with small discrepancies. The beam current was kept around 10 nA in order to avoid large dead time corrections in the collected gamma spectra (achieved below 2%). Gamma-ray detection was accomplished using a 45% Ge(HP) detector (nominal energy resolution of 2.2 keV at 1173 keV) placed at an angle of 135° with respect to the beam axis. The detector's absolute efficiency was determined using radioactive sources, namely ^{133}Ba and ^{152}Eu, placed at the position of the samples [40].

Pole figures were obtained using X-ray diffraction analysis employing a Bruker – AXS D8 Disvover and using the Cu $K_{\alpha1,2}$ lines collimated with a Gobël mirror, a Ni filter and a 1.5 mm slits. Data were collected using a scintillation detector and a 0.2 mm antiscattering slit in order to avoid the effect of the grain orientation.

3. Results and discussion

Three ingots of $Ga_{0.8}In_{0.2}Sb$ ternary alloy were obtained under identical growth conditions: the ingot B, which was undoped, and ingots E and F which were doped with aluminum. Despite the lower concentration of Al in the samples, it was possible to identify and quantify all samples (Table 1). To quantify the Al present in the $Ga_{0.8}In_{0.2}Sb$:Al samples, we used the ERYA code [39], which integrates the nuclear reaction excitation function of the 27Al(p,p′γ)27Al nuclear reaction along the depth of the sample.

Fig. 2 shows a spectrum corresponding to the end sample of ingot E. Several gamma-lines are observed in the presented gamma-energy range, being the most dominant the 175 keV, from

Table 1
Average composition of radial samples obtained by PIXE. Al concentration was obtained by PIGE.

Average composition by PIXE and PIGE				
Samples	%at.			
	Ga	In	Sb	Al
B_beginning	46.6	3.8	49.6	–
B_middle	42.5	6.4	51.1	–
B_end	29.5	20.5	50.0	–
E_beginning	36.2	8.7	55.0	0.002
E_middle	34.3	10.7	55.0	0.002
E_end	30.5	14.7	54.8	0.027
F_beginning	37.4	6.4	56.2	0.021
F_middle	36.4	7.8	55.8	0.002
F_end	35.2	9.8	55.0	0.007

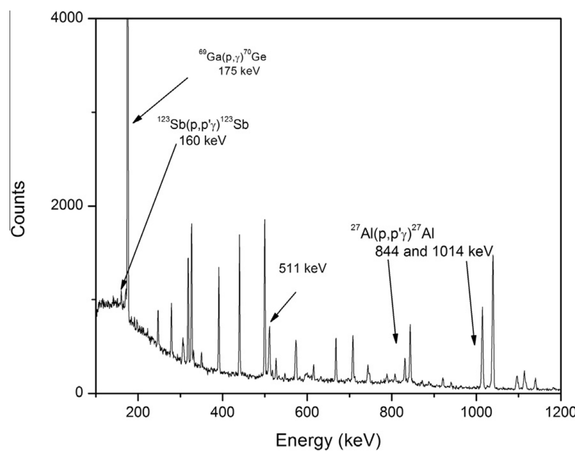

Fig. 2. PIGE spectrum from the end part of the ingot E.

the 69Ga(p,g)70Ge nuclear reaction. The 844 keV and the 1014 keV gamma-lines come from the reaction 27Al(p,p′g)27Al. The relevant gamma-ray lines are well separated from other lines, with a consequent small uncertainty for area extraction.

Fig. 3 shows the SEM/BSE images recorded along the growth direction of the ingots, from the beginning to the end. All images for the ingot B show a compositional distribution strongly inhomogeneous with presence of grains, twins and small Sb-rich precipitates (∼10–80 μm), which in some cases have up to 88 at.% of Sb. Ingot E (doped) presents a better homogeneous composition and lower defect concentration when compared with ingot B (undoped). The presence of defects, mainly grains and Sb-rich precipitates, increases along the growth direction. Ingot F also presents a small compositional variation when compared with the ingot B (undoped), and also shows more precipitates, grains and twins at the end of the ingot. It is observed that this ingot F, as ingot B, has small precipitates (∼10–100 μm) with large amounts of the Sb (in some cases up to 93.2 at.%).

EDS analyses performed along the growth direction (steps of 1 mm) allow us to have information about the In distribution in the ingots. For the undoped ingot, the In concentration was much higher in the end and the segregation coefficient obtained for this ingot was about $k_{eff} = 0.32$. On the other hand, the In distribution in the doped crystals is more homogeneous and the segregation coefficient obtained is slightly lower than 1 ($k_{eff} = 0.91$ for ingot E and $k_{eff} = 0.80$ for ingot F), thus the In concentration increases smoothly along the growth direction. These results suggest that the presence of Al in the ternary alloy promotes not only a better distribution of the different elements involved, mainly the indium, originating a more homogeneous composition throughout the ingot solidification direction, but also reduces the concentration of precipitates.

The three ingots were grown under similar conditions, therefore the same behavior was expected for the doped ingots (E and F). However, differences were observed by EDS/SEM images and may be related to sensitivity of the growth process. Factors such as fluctuations of furnace power supply and the rejection of indium may have occurred during the growth, thus causing the

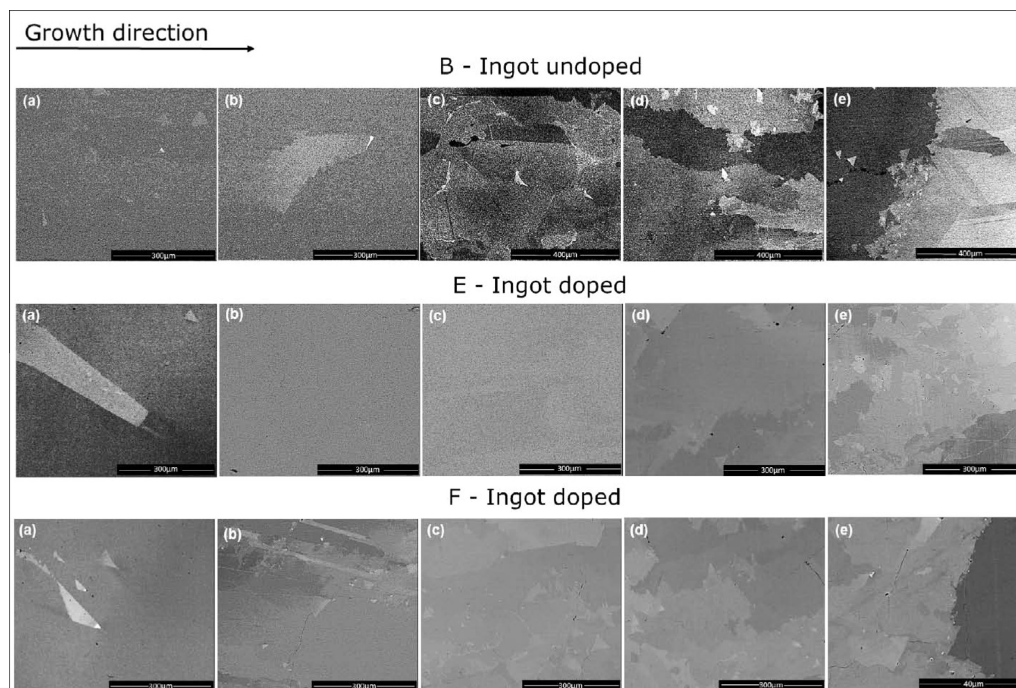

Fig. 3. SEM/BSE images along the growth direction of the ingots B ($Ga_{0.8}In_{0.2}Sb$), E ($Ga_{0.8}In_{0.2}Sb$:Al) and F ($Ga_{0.8}In_{0.2}Sb$:Al). (a) Beginning. (b–d) Middle. (e) End.

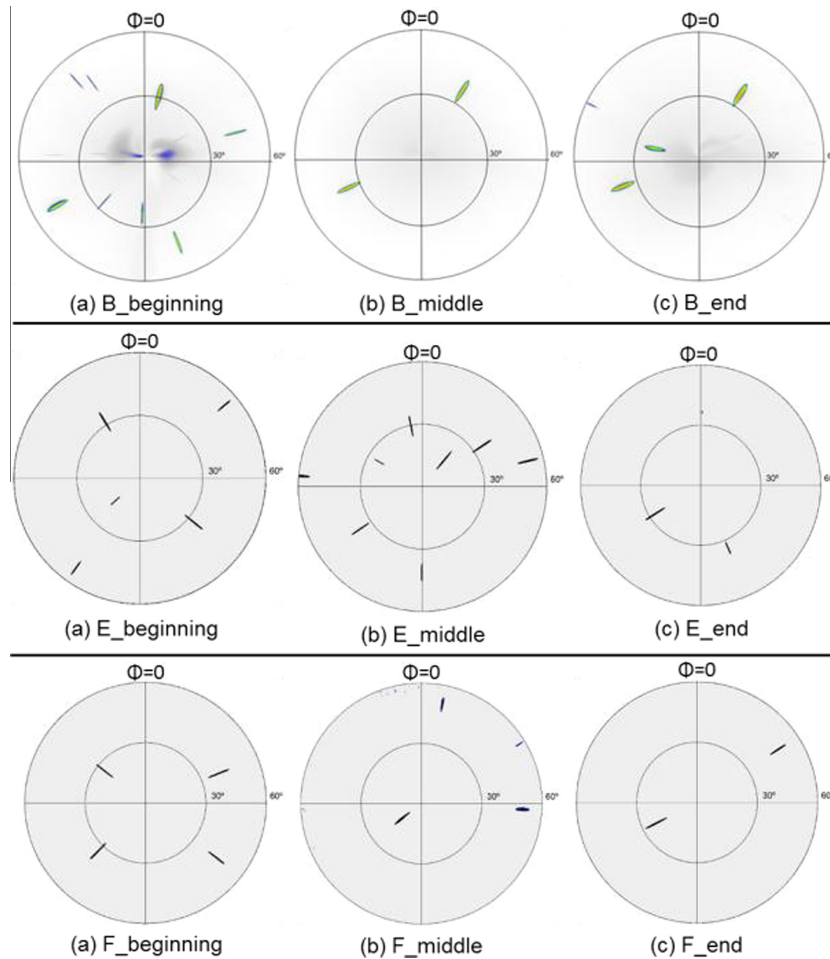

Fig. 4. Pole figures along the (1 1 1) direction for undoped and doped ingots.

constitutional supercooling that lead to a shift in the solid–liquid interface and resulting in changes on grain size and increase of heterogeneous regions such as those observed in the ingot F.

The crystalline quality in the radial samples of ingots can be seen by pole figures along the (1 1 1) direction presented in Fig. 4. In these alloys, the (1 1 1) direction is the preferential growth direction, meeting the direction requirement in device technologies for large-scale applications [10]. In general, the higher concentration of grains is found at the beginning of the ingots which is related to the ampoule shape (cone) and the competition of grains at this early stage of the growth. It can be also observed that the number of grains oriented towards the (1 1 1) direction is lower when the samples are doped with Al, especially at the beginning of the body and at the end of each ingot. It is also remarkable that some of the grains observed at the beginning or at the middle of the crystals are also present at the end. This fact shows that despite the possible instabilities happened along the growth process, it was possible to maintain a high degree of crystallinity along the growth direction.

The average composition of these radial samples (different positions were measured along the surface of the samples with a broad proton beam) was obtained by PIXE and the results are shown in Table 1.

Observing the data shown in Table 1 it is noted that doped ingots show a Sb enrichment when compared with undoped ingots and also for the three ingots, the indium concentration increases along the growth direction, being higher at the end of the ingot, although less pronounced in the doped ingots (similar behavior was observed by EDS measurements). Considering the ingot E, both Al and In concentration increase towards the end of the ingot. This result was not expected for the aluminum, since it has a segregation coefficient $k_o > 1$ [21]. However, this behavior has resulted in a more homogeneous and surface free of precipitates and defects (Fig. 3) ingot, with a segregation coefficient for the In very close to the unity. On the other hand, the Al distribution in ingot F is higher at the beginning, which did not preclude the In segregation at the end, and the SEM images showed a more heterogeneous surface.

When analyzing the pole figure with the presence of Al, referring to the middle samples of ingot E and F, it is emphasized the possibility of variation during the growth process because the amount of Al is the same but the presence of grains in sample E is higher, which is possibly related to the In segregation.

Regarding the middle samples of the doped ingots, with similar concentration of aluminum, the Sb concentration is similar between them and higher than the concentration in the undoped sample, suggesting that the aluminum promotes a more uniform distribution of the elements along of the $Ga_{0.8}In_{0.2}Sb$ crystals.

4. Conclusions

The segregation behavior of indium in undoped and aluminum doped $Ga_{0.8}In_{0.2}Sb$ ingots was studied and the results indicate that the indium is distributed more homogeneously in the doped than in the undoped ingots, affecting also the concentration of Ga and Sb. All the ingots of GaInSb obtained exhibit defects such as twins,

Sb-rich precipitates and grains, which are higher in the undoped ingot. The GaInSb:Al samples show a indium segregation coefficient close to one, suggesting, that the presence of aluminum fosters a better distribution of the indium and lower concentration of precipitates and defects, especially at the middle of the ingots.

Even at very low concentration, it was possible to identify and quantify Al in all samples by PIGE, but the distribution is not uniform along the growth direction.

More studies will be performed to fully understand the behavior of Al along the growth direction and to control it, in order to control also the In distribution and improve the compositional homogeneity of these alloys.

Acknowledgments

This work was carried out within the contract CAPES Proc. No. 026612-4 together with CTN/IST. V. Corregidor acknowledges FCT for the Ciência program. The work was partially supported by FCT-Portugal (PEST-OE/FIS/UI0275/2011), *CNPQ/CAPES No. 06/2011 – CASADINHO/PROCAD* – (*No.*: *552415/2011-1*). The InSb alloy was donated from Research Institute of Electronic, Shizuoka University, Japan.

References

[1] J. Vincent, E. Diéguez, Microstructure and solidification behavior of cast GaInSb alloys, J. Cryst. Growth 295 (2006) 108.
[2] B.R. Bennett et al., Antimonide-based compound semiconductors for electronic devices: a review, Solid-State Electronics 49 (2005) 1875.
[3] P.S. Dutta, III–V ternary bulk substrate growth technology: a review, J. Cryst. Growth 275 (2005) 106.
[4] M. Henini, M. Razzeghi, Handbook of Infra-red Detection Technologies, Elsevier, 2002. 532 p.
[5] C. Liu, Y. Li, Y. Zeng, Progress in antimonide based III–V compound semiconductors and devices, Engineering 2 (2010) 617.
[6] H.X. Yuan, D. Grubisic, T.T.S. Wong, GaInSb photodetectors developed from single crystal bulk grown materials, J. Electron. Mater. 28 (1999).
[7] C. Stellian, T. Duffar, A. Mitric, V. Corregidor, L.C. Alves, Barradas, Growth of concentrated GaInSb alloys with improved chemical homogeneity at low and variable pulling rates, J. Cryst. Growth 283 (2005) 124.
[8] P.S. Dutta, V. Kumar, The physics and technology of gallium antimonide: an emerging optoeletronic material, J. Appl. Phys. 81 (1997) 5821.
[9] P.S. Dutta, A.G. Ostrogorsky, Segregation of Ga in Ge and InSb in GaSb, J. Cryst. Growth 217 (2000) 360.
[10] P.S. Dutta, Bulk growth of crystals of III–V compound semiconductors, Compr. Semicond. Sci. Technol. 3 (2011) 36.
[11] N. Murakami et al., Growth of homogeneous InGaSb ternary alloy semiconductors on InSb seed, J. Cryst. Growth 310 (2008) 1433.
[12] H.J. Kim, A. Chandola, R. Bhat, P.S. Dutta, Forced convection induced thermal fluctuations at the solid–liquid interface and its effect on the radial alloy distribution in vertical Bridgman grown $Ga_{1-x}In_xSb$ bulk crystals, J. Cryst. Growth 289 (2006) 450.
[13] J. He, S. Kou, Liquid-encapsulated Czochralski growth of $Ga_{1-x}In_xAs$ single crystals with uniform compositions, J. Cryst. Growth 308 (2007) 10.
[14] A. Mitric, Th. Duffar, A. Amariei, X. Chatzistavrou, E. Pavlidou, K.M. Paraskevopoulos, E.K. Polychroniadis, On the synthesis and characterization of polycrystalline GaSb suitable for thermophotovoltaic (TPV) applications, J. Optoelectron. Adv. Mater. 7 (2) (2005) 659.
[15] G. Rajesh, M. Arivanandhan, H. Morii, T. Aoki, T. Koyama, Y.A. Momosea, A. Tanaka, T. Ozawa, Y. Inatomi, Y. Hayakawa, In-situ observations of dissolution process of GaSb into InSb melt by X-ray penetration method, J. Cryst. Growth 312 (2010) 2677.
[16] B.C. Houchens, P. Becla, S.E. Tritchler, J.A. Goza, D.F. Bliss, Crystal growth of bulk ternary semiconductors: comparison of GaInSb growth by horizontal Bridgman and horizontal traveling heater method, J. Cryst. Growth 312 (2010) 1090.
[17] B. Chalmers, Transient solute effects crystal growth of silicon, J. Cryst. Growth 82 (1987) 70.
[18] C. Barat, T. Duffar, P. Dusserre, J.P. Garandet, Chemical segregation in vertical Bridgman growth of GaInSb alloys, Cryst. Res. Technol. 34 (1999) 449.
[19] B.A. Dedavid, Estudo na Influência do Alumínio como Dopante e do Ultra-Som em Lingotes de Antimoneto de Gálio Crescidos por LEC (Tese, Doutorado em Engenharia), Universidade Federal do Rio Grande do Sul, Porto Alegre, Brasil, 1994, 154 p.
[20] A.F. Witt, T. Jasinski, On control of the crystal-melt interface shape during growth in a vertical Bridgman configuration, J. Cryst. Growth 71 (1985) 295.
[21] E.M. Costa, B.A. Dedavid, A. Muller, Investigations of structural defects by etching of GaSb grown by the liquid-encapsulated Czochralski technique, J. Mater. Sci. Eng. B B44 (1997) 208.
[22] M. Haris, Y. Hayakawa, F.C. Chou, P. Veeraamani, S. Morthy Babu, Structural, compositional and optical analysis of $InAs_xSb_{1-x}$ crystals grown by vertical directional solidification method, J. Alloys Compd. 548 (2013) 23.
[23] M. Nobeoka, Y. Takagi, Y. Okano, Y. Hayakawa, S. Dost, Numerical simulation crystal growth by temperature gradient method under normal- and micro-gravity fields, J. Cryst. Growth 285 (2014) 66.
[24] A.G. Ostrogorsky, A. Marin, A. Churilov, M.P. Voz, W.A. Bonner, T. Duffar, Reproducible Te-doped InSb experiments in Microgravity Science Glovebox at the International Space Station, J. Cryst. Growth 310 (2008) 364.
[25] K. Kinoshita, H. Kato, S. Matsumoto, S. Yoda, Growth of homogeneous $In_{1-x}GaSb$ crystal by the graded solute concentration method, J. Cryst. Growth 216 (2000) 37.
[26] J. Vincent, Bermudez, E. Dieguez, L.C. Alves, V. Corregidor, N.P. Barradas, Comparison between vertical Bridgman and feeding techniques for GaInSb alloy growths, J. Cryst. Growth 275 (2005) e537.
[27] V. Corregidor, E. Alves, L.C. Alves, N.P. Barradas, Th. Duffar, N. Franco, C. Marques, A. Mitric, Compositional and structural characterization of GaSb and GaInSb, Nucl. Instr. Meth. Phys. Res. B 240 (2005) 360.
[28] A. Mitric, T. Duffar, V. Corregidro, L.C. Alves, N.P. Barradas, Growth concentration alloys under alternating magnetic field, J. Cryst. Growth 310 (2008) 1424.
[29] S.C. Tsaur, S. Kou, Czochralski Growth of $Ga_{1-x}In_xSb$ single crystals with uniform compositions, J. Cryst. Growth 307 (2007) 268.
[30] C. Díaz-Guerra et al., Cathodoluminescence mapping and spectroscopy of Te-doped $In_xGa_{1-x}Sb$ grown by vertical Bridgman method under an alternative magnetic field, Superlattices Microstruct. 45 (2009) 407.
[31] G.N. Kozhemyakin, L.V. Nemets, A.A. Bulankina, Simulation of ultrasound influence on melt convection for the growth of $Ga_xIn_{1-x}Sb$ and Si single crystals by the Czochralski method, Ultrasonics 54 (2014) 2165.
[32] D. Bliss, P. Becla, Growth and characterization of bulk GaInSb crystals from nonstoichiometric melts, International Conference on Indium Phosphide and Related Materials, vol. 20, 2008, Versailles, Conference Publications, IPRM, Versailles, 2008.
[33] A. Dario, H.O. Sicim, E. Balikci, A new approach for dopant distribution and morphological stability in Crystal grown by the axial heat processing (AHP) technique, J. Cryst. Growth 337 (2011) 65.
[34] P. Hidalgo, B. Méndez, J. Piqueras, P.S. Dutta, E. Dieguez, Decoration of extended in GaSb by Al doping as evidenced by cathodoluminescence studies, Solid State Commun. 108 (1998) 997.
[35] B. Krishan et al., Growth of $Ga_xIn_{1-x}Sb$ bulk crystals for infrared devices applications by vertical Bridgman technique, Mater. Lett. 58 (2004) 1441.
[36] Fernandes, Kendra D'Abreu Neto, Segregação do índio em lingotes $Ga_{(1-x)}In_xSb$ obtidos pelo método Bridgman vertical (Dissertação, Mestrado em Engenharia e Tecnologia de Materiais), 2012, Programa de Pós-Graduação em Engenharia e Tecnologia de Materiais, Pontifícia Universidade Católica do Rio Grande do Sul, Porto Alegre, 2012.
[37] M. Streicher, Influence of Aluminum on Segregation Behavior of Indium in Ternary Alloys of $Ga_{(1-x)}In_xSb$ (Ph.D. thesis, Graduation Program in Materials Engineering and Technology), Pontificial Catholic University of Rio Grande do Sul, Brazil, 2015.
[38] J.A. Maxwell, W.J. Teesdale, J.L. Campbell, The Guelph PIXE software package II, Nucl. Instr. Meth. Phys. Res., Sect. B: Beam Interact. Mater. Atoms 95 (1995) 407.
[39] R. Mateus, M. Fonseca, A.P. Jesus, H. Luís, J.P. Ribeiro, Nucl. Instr. Meth. B 229 (2005) 302.
[40] R. Mateus, A.P. Jesus, J.P. Ribeiro, Nucl. Instr. Meth. Phys. Res. B 266 (2008) 1490.